forests

MDPI

Article

Simulating Ecological Functions of Vegetation Using a Dynamic Vegetation Model

Yanli Su [1], Jielin Zhang [1], Shouzhang Peng [2,*] and Yongxia Ding [3]

[1] College of Natural Resources and Environment, Northwest A&F University, Xianyang 712100, China
[2] State Key Laboratory of Soil Erosion and Dryland Farming on the Loess Plateau, Northwest A&F University, Xianyang 712100, China
[3] Shaanxi Key Laboratory of Disasters Monitoring & Mechanism Simulation, College of Geography and Environment, Baoji University of Arts and Sciences, Baoji 721013, China
* Correspondence: szp@nwafu.edu.cn; Tel.: +86-131-5200-7691

Abstract: The ecological functions of vegetation play a significant role in improving human well-being. However, previous studies on ecological functions have only used semi-empirical models, which do not include physiological mechanisms and therefore do not accurately estimate the ecological functions of vegetation under scenarios of future climate change. To address this problem, a process-based dynamic vegetation model (LPJ-GUESS) was used to simulate the ecological functions of vegetation under different climate change scenarios in the Loess Plateau (LP), a typical ecologically fragile area in China. The simulated ecological functions were the carbon stock function (CS), soil conservation function (SC), and the water conservation function (WC). The results showed that: (1) Compared with 2001–2020, the proportion of area by shrub and grass vegetation that was predicted to transform into forest accounted for more than 1% of the area in the LP under the SSP119 scenario and 3% of the area in the LP under the SSP585 scenario during 2081–2100, respectively. (2) Compared with 2001–2020, the CS would decrease in the central and south-eastern regions, the SC would decrease in the western regions, and the WC would decrease in the Qilian, Wushaoling, Xinglong and Liupan Mountains during 2081–2100. (3) The relationships and the corresponding regions between the ecological functions of the vegetation and the corresponding regions in the LP would change significantly under climate change from 2001–2020 to 2081–2100.These results indicate that a process-based dynamic vegetation model can capture the changes in the carbon and water fluxes under changes in the climate and CO_2 concentration. It can also capture the vegetation succession, changes in ecological functions, and the transformation of functional relationships, which provide information that is conducive to the management and restoration of vegetation on the LP. This study supplies a novel perspective for vegetation management and high-quality development in other ecologically fragile regions worldwide.

Keywords: carbon stock; soil conservation; water conservation; LPJ-GUESS model; Loess Plateau

check for updates

Citation: Su, Y.; Zhang, J.; Peng, S.; Ding, Y. Simulating Ecological Functions of Vegetation Using a Dynamic Vegetation Model. *Forests* **2022**, *13*, 1464. https://doi.org/10.3390/f13091464

Academic Editor: Juan A. Blanco

Received: 16 July 2022
Accepted: 7 September 2022
Published: 11 September 2022

Publisher's Note: MDPI stays neutral with regard to jurisdictional claims in published maps and institutional affiliations.

Copyright: © 2022 by the authors. Licensee MDPI, Basel, Switzerland. This article is an open access article distributed under the terms and conditions of the Creative Commons Attribution (CC BY) license (https://creativecommons.org/licenses/by/4.0/).

1. Introduction

Ecosystem services refer to all of the benefits that human beings obtain from the ecosystem [1]. The Millennium Ecosystem Assessment [2] identified regulating services as one of the least understood but potentially the most valuable services provided by ecosystems, primarily in the context of research on ecological functions in ecologically fragile areas. The ecological functions of vegetation play a vital role in improving the environment, alleviating global warming, and improving human welfare. Studies on the ecological functions of vegetation have important scientific value for future vegetation management, with land use and climate change playing a key role in changing ecosystem services [3]. The IPCC Sixth Assessment Report made a systematic assessment of the potential changes in global surface temperature and precipitation in the 21st century. The

assessment highlighted that the average global surface temperature will increase by at least 1.5 °C in the next 20 years. The average precipitation will also increase according to the season, and it will vary by region. Climate change will continue to affect the carbon–water cycle and vegetation structure, which has a considerable impact on ecological functions and may also affect the transformation of the relationships between ecological functions [4]. Further research on dynamic changes in vegetation ecological functions under climate change at the global scale is an urgent priority, as is providing climate adaptation strategies for future vegetation management and the improvement of ecological functions.

Studies on the ecological functions under climate change have been undertaken worldwide [5–8]. However, these studies mainly predict future land use scenarios based on CA-Markov models and analyze spatial changes in ecosystem services combined with InVEST models. These studies have not clearly described dynamic changes in the vegetation and the interaction between climate, soil, CO_2 concentrations, and the vegetation [9]. Therefore, there is considerable uncertainty in predicting the carbon and water flux and the vegetation structure. This is because current research methods for examining ecological functions are limited. For example, the InVEST model is a semi-empirical model that is mainly used for the comprehensive evaluation of ecosystem services and trade-offs; however, it lacks a description of the mechanisms and processes of dynamic change in the vegetation ecosystem [10]. Therefore, it cannot effectively simulate vegetation succession, the carbon and water cycles, or the vegetation structure under climate change. The dynamic vegetation model can simulate the carbon and water flux, which can be used alongside its structure to estimate or calculate ecological functions. In this type of research, the dynamic vegetation model is recommended to simulate the vegetation pattern as well as ecological function patterns and relationships under future climate change.

Process-based dynamic vegetation models can quantify the dynamics of ecosystem services under climate change and their related policy scenarios, and reflect the relationships between ecosystem services [11]. Process-based dynamic vegetation models can examine many climatic vegetation mechanisms such as leaf transpiration, soil evaporation, photosynthetic respiration, competition, death, community succession, and canopy structure dynamics. They have many applications in response to vegetation carbon and water fluxes and their structure under climate change [12]. At present, the common dynamic vegetation models include LPJ-DGVM (Lund–Potsdam–Jena Dynamic Global Vegetation Model) [13], SEIB-DGVM (Spatially Explicit Individual-Based Dynamic Global Vegetation Model) [14] and LPJ-GUESS (Lund–Potsdam Jena Universal Ecosystem Simulator) [15]. LPJ-GUESS is an updated edition of the LPJ-DGVM model that refines the simulation at the individual plant level. This makes the dynamic simulation of vegetation composition, structure, and function more accurate [12]. The LPJ-GUESS model can not only be used to examine the mechanisms of large-scale vegetation dynamics, but it has also been used to introduce gap model and patch concepts to refine vegetation dynamics. This includes the vegetation succession, species composition and density, and changes in the community morphological structure. Driven by monthly climate data, annual atmospheric CO_2 concentration data, soil data, and vegetation eco-physiological parameters, vegetation dynamics can be simulated and analyzed at the typical plant functional type (PFT) level. The community structure and its response to climate change can be predicted according to the preset composition of PFTs [16], so it has been universally used in vegetation research [16–19].Therefore, the LPJ-GUESS model may be a powerful tool for implementing research on the ecological functions of vegetation under future climate change.

The Loess Plateau (LP) is situated in the north of China and is a transition zone from a semi-humid to semi-arid climate, with the vegetation ecosystem being highly sensitive to climate change. The vegetation distribution sequence from the southeast to the northwest is the forest zone, the forest–grass transition zone, and the grass zone. The vegetation distribution shows a distinct zonal trend, and the vegetation system has a simple structure, low productivity [20], dry soil, and water shortages [21], resulting in a fragile ecological environment. Many studies have assessed historical ecological functions [22–27],

and the examination of examining future changes has based on ca-Markov models to predict land use change scenarios, and estimate ecological functions under future scenarios. However, these studies have predominantly excluded investigation into the dynamic impacts of climate change on vegetation structure. Furthermore, the prediction of the dynamic evolution of ecological functions under climate change is insufficiently accurate. Temperature and precipitation in the LP will increase and fluctuate considerably in the future, indicating a pronounced climate response to global warming in the region [28]. Therefore, the LP is an ideal research area to study the dynamic evolution of ecological functions of vegetation under climate change, with findings that hold the potential to improve the ecological environment in the region.

Accordingly, taking the LP as the study area, the aim of this study were to verify the suitability of the LP-GUESS model for modelling the response of vegetation to climate change, and to use the model to simulate the changes in the vegetation distribution and ecological functions. Specifically, the spatiotemporal changes for the vegetation types and ecological functions were analyzed under two climate change scenarios during 2001–2020 and at the end of this century (2081–2100). Accordingly, vegetation management strategies to support climate change adaptation are proposed. We hope the approach of this study will provide insight into predicting future vegetation functions in other regions of world.

2. Materials and Methods

2.1. Study Area

The LP is situated in northern China, covering an area of approximately 640,000 km^2 (Figure 1). The terrain descends in waves from the northwest to the southeast. There is a high level of surface undulation, with the elevation and ground slopes ranging from 200 m to 3000 m and 15° to 30°, respectively. The LP is in the transition zone between the humid monsoon climate in southeast China and the arid climate in northwest China. The mean annual temperature is 4.3–14.3 °C, and the daily temperature also greatly fluctuates, with high temperatures and rainfall during the summer and cold and dry conditions in the winter. The precipitation is mainly concentrated during July–September, accounting for 60–80% of the annual precipitation. The winter precipitation accounts for approximately 5%, with evaporation is generally being higher than the precipitation [29,30]. The spatial area of soil and water loss is 45.4 × 10^4 km^2, making it the area with the most severe soil and water loss and the most vulnerable ecology in China and worldwide [31].

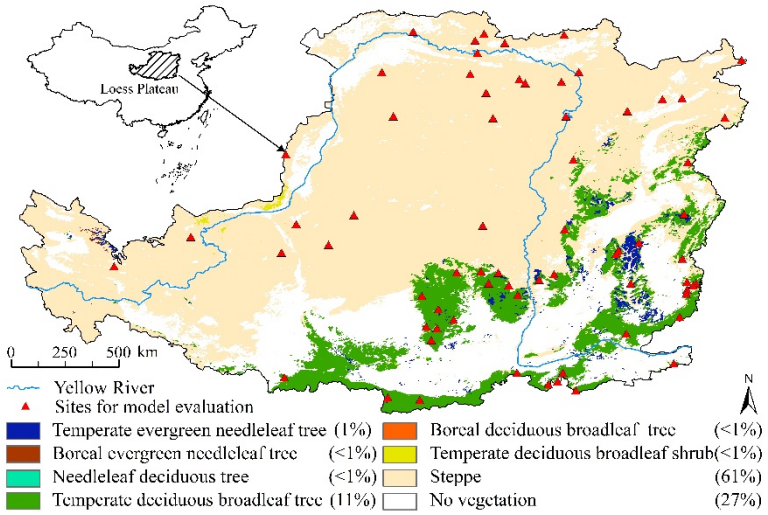


Figure 1. Location of current typical vegetation types and the sites used for model evaluation of the Loess Plateau.

2.2. Data Collection

In this study, the LPJ-GUESS model was used to simulate the spatial pattern and ecological functions of vegetation on the LP. The input data for LPJ-GUESS were the PFT data, climate data (monthly average temperature, total precipitation, and the average cloud cover), CO_2 concentration, soil texture, and the eco-physiological parameters of the vegetation [32]. The PFT data were sourced from the MODIS products official website (https://lpdaac.usgs.gov/products/mcd12c1v006/) (accessed on 9 November 2020), and the climate data from 2001 to 2100 were obtained from the National Geographic Resource Science Sub Center, National Earth System Science Data Center, National Science & Technology Infrastructure of China (http://gre.geodata.cn) (accessed on 9 November 2020). Specifically, 2001–2020 was the historical period, and 2021–2100 was the future period. The projected climate data for 2021–2100 were based on the newly released IPCC Shared Socio-economic Path scenarios (SSP119 and SSP595), each of which contain three General Circulation Models (GCMs) (EC-Earth3, GFDL-ESM4 and MRI-ESM2-0) that perform well in predicting future climate change in China [32]. These GCMs were constructed by the European Community-Earth Alliance, the American Geophysical Fluid Mechanics Laboratory, and the Japan Meteorological Research Institute. Scenarios SSP119 and SSP585 correspond to a low forcing, low greenhouse gas emission scenario and a high forcing, high greenhouse gas emission scenario, respectively. Therefore, the future ecological functions of vegetation under the SSP119 and SSP585 scenarios can indicate the possible range of future climate change. The simulation results were based on the mean of the three GCMs to reduce possible instability caused by the climate scenarios. Data on current and future CO_2 concentrations came from the Mauna Loa Observatory (https://scrippsco2.ucsd.edu/) (accessed on 9 November 2020) and the SSP datasets (https://tntcat.iiasa.ac.at/SSPDb) (accessed on 9 November 2020), respectively [32,33]. Soil texture data were obtained from the Global Soil Data Center (http://soilgrids.org) (accessed on 9 November 2020). Vegetation distribution data in the LP and the bioclimatic variables used to determine the LP bioclimatic and eco-physiological parameters were obtained from the Loess Plateau Science Data Center (http://loess.geodata.cn/) (accessed on 9 November 2020) and the National Ecological Science Data Center (http://www.cnern.org.cn/) (accessed on 9 November 2020).

2.3. Model Simulation

LPJ-GUESS is a multi-scale dynamic vegetation model that simulates the biomass, gross primary productivity (GPP), leaf area index (LAI), and evapotranspiration (ET) of the vegetation in an ecosystem [15]. It can reasonably simulate the continuous evolution of the spatiotemporal patterns of vegetation and its ecological functions under a changing climate and atmospheric CO_2 concentration.

Although the development team of the LPJ-GUESS model stressed that the proposed parameters could be used to model the vegetation dynamics in different regions worldwide [15], this study aimed to identify the parameters for PFTs to accurately simulate the vegetation spatial distribution of the LP. In this model, 57 ecological and physiological parameters needed to be identified for each PFT. This study used data analysis to directly determine the values for four bioclimatic parameters that determine the distribution of PFTs. The distribution and biological climate data were spatially overlaid to extract bioclimatic parameters for each vegetation type, such as the minimum and maximum temperatures for the coldest and the warmest months, as well as temperatures greater than 5 °C [32]. Vegetation sampling points were obtained through field investigation. In this study, the ecological physiology parameters analyzed included the maximum canopy area, wood density, the carbon and nitrogen contents of fine root and sapwood, and other eco-physiological parameters referred to the same or similar PFTs in the parameters for existing research models. For the remaining 53 parameters, according to the literature [34], 21 parameters are considered to be sensitive parameters [16] (Table S1). Therefore, in this study, a genetic algorithm was developed in the MATLAB language environment, focusing on the calibration of these sensitive parameters. Considering the integrity of the LPJ-GUESS

model in simulating carbon and water fluxes and the spatial distribution of vegetation, the vegetation parameters were calibrated jointly with multi-source measurements to ensure that they were representative of the study area.

The model simulations were carried out one by one on a 1 km resolution grid. The parameter-calibrated LPJ-GUESS model cycled CO_2 concentration and climate data for each geographic grid during 2001–2020, starting with the PFT data for the LP in 2019, to drive the carbon and nitrogen pools of vegetation/soil to a state of dynamic equilibrium. In this state, the carbon and nitrogen values were taken as the starting conditions of each grid and were combined with the CO_2 concentration and climate data (2001–2020, 2021–2100). The biomass, GPP, LAI, and ET of the vegetation were continuously simulated across annual time scales. The vegetation type in each grid was determined by the biomass in the grid, and the detailed classification of the vegetation type in the grid was based on our previous studies [17]. The GPP, ET, and LAI of the vegetation in each grid were used to represent or calculate the carbon stock (CS), soil conservation (SC), and water conservation (WC), respectively.

To evaluate the accuracy of the LPJ-GUESS model in simulating the GPP, ET, and LAI of the LP, we selected 51 natural vegetation points through field investigation (Figure 1). The sampling points were extracted from the corresponding MODIS products (https://modis.gsfc.nasa.gov/) (accessed on 5 December 2021) during 2001–2020 according to their geographical location, including the GPP, ET, and LAI values. The annual remote sensing observation data extracted from the MODIS products were fitted linearly with the data simulated from 2001 to 2020 by the LPJ-GUESS model. The average coefficient of determination (r^2) and the average Nash–Sutcliffe Efficiency (Ens) between the observed and simulated values of GPP, ET, and LAI were 0.77 and 0.53, respectively. In this study, acceptable model performance was considered when $r^2 > 0.6$ and Ens > 0.5 [35] (Figure 2).

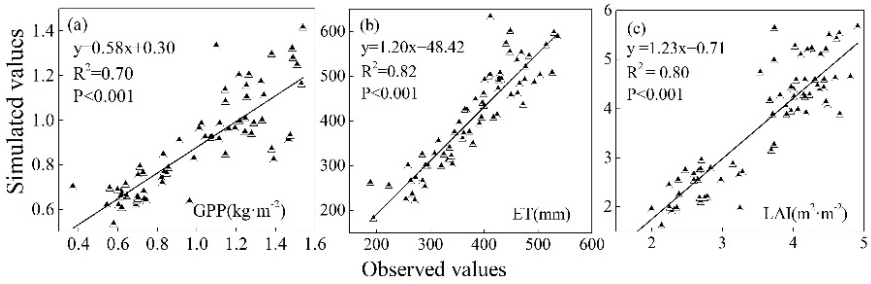


Figure 2. Comparisons between the observed (x) and simulated (y) values of annual (**a**) gross primary productivity (GPP), (**b**) evapotranspiration (ET), and (**c**) leaf area index (LAI) of the Loess Plateau from 2001 to 2020.

The vegetation spatial pattern was determined using the classification criteria of Wolf et al. [36]. The specific classification details are shown in Table 1. Based on the biomass simulated by the model and according to the proportion of vegetation biomass of woody plants and other growth forms (Table 1), the LP vegetation types were divided into forest, shrub, grass, and bare land.

Table 1. Classification of vegetation types based on the LPJ-GUESS model.

Number	Vegetation Types	Model Classification
1	Forest	>85% of biomass consists of woody species and 75% of those are forest
2	Shrub	>50% of biomass is shrub
3	Grass	>50% of the biomass is grass
4	Bare Land	biomass < 0.02 $kg \cdot m^{-2}$

2.4. Calculation of Ecosystem Service Functions

Referring to related studies on the ecological effects of vegetation on the LP [37], the ecological effects of vegetation on the LP was calculated based on the annual average SC, CS, and WC.

The average annual SC of the vegetation (ΔA, t·ha^{-1}yr^{-1}) was calculated based on the soil loss equation [38], as follows:

$$\Delta A = R \times K \times L \times S \times (1 - C \times P) \quad (1)$$

where R is the rainfall erosivity factor (MJ·mm·ha^{-1}·h^{-1}·yr^{-1}), calculated using downscaled monthly precipitation data.

$$R = \sum_{1}^{12} \left(1.735 \times 10^{(1.5 \log_{10}(\frac{pi^2}{p}) - 0.8188)} \right) \quad (2)$$

where pi represented the monthly average precipitation, p represents the average annual precipitation, and K is the soil erodibility (t·ha^{-1}·h·ha^{-1}·MJ^{-1}·mm^{-1}). The data were obtained from the National Geographic Resource Science SubCenter, National Earth System Science Data Center, National Science & Technology Infrastructure of China (http://www.geodata.cn) (accessed on 15 May 2021). L and S are the slope length factor and slope factor, respectively, based on the digital elevation model data of the study region, which were obtained using the terrain factor calculation tool. C is the cover-management factor, which was quantified according to its mathematical relationship with the simulated LAI and the vegetation coverage [39]:

$$\begin{cases} C = 1 & f_c = 0 \\ C = 0.6508 - 0.3436 \lg f_c & 0 < f_c < 78.3\% \\ C = 0 & f_c \geq 78.3\% \end{cases} \quad (3)$$

where fc is the vegetation coverage:

$$f_c(\theta) = 1 - e^{-G(\theta) LAI / \cos\theta} \quad (4)$$

$G(\theta)$ is the projection of the leaves in the incident direction of the sun, which characterized the light interception ability of the leaves; θ is the incident zenith angle of the sun. When the vegetation leaves are randomly distributed in a spherical shape, $G(\theta) = 0.5$. By simulating the LAI, the vertical vegetation coverage of forest, shrub, and grass can be accurately estimated [40]. P is the support practice factor, which was assigned a value of 1 in this study [39].

The CS of the vegetation was calculated using the GPP data (kg·m^{-2}) of the model simulation results.

Soil moisture was negligible when calculating the multi-year mean water conservation (WC) (mm), which was quantified by the following formula [41]:

$$WY = P - ET \quad (5)$$

where P is the annual average precipitation, calculated using monthly precipitation data, and ET is the result simulated by the model.

2.5. Relationships of Ecosystem Service Functions

The partial correlation coefficient was used to calculate the correlation between ecological functions, which can eliminate the influence between other variables. Correlations between ecological functions included synergistic and trade-off relationships, and they were superimposed to identify areas where the relationship between functions changed.

The partial correlation coefficients between the CS, SC, and WC in each grid were calculated according to formula (6):

$$r_{12(3)} = \frac{r_{12} - r_{13}r_{23}}{\sqrt{1 - r_{13}^2}\sqrt{1 - r_{23}^2}} \quad (6)$$

where an r value greater than zero indicates a synergistic relationship, and less than zero indicates a trade-off relationship [42]. Significance was expressed at the 95% confidence level in this study.

3. Results

3.1. Spatiotemporal Change in Vegetation Types under Climate Change

During 2081–2100, the vegetation distribution on the LP showed distinct spatial heterogeneity (Figure S1), where forests were mainly centered in the south and southeast, accounting for 10% of the total area in the LP under the SSP119 scenario, and 11% of the total area in the LP under the SSP585 scenario. (Table S2). Grasses were mainly centered in the north and northwest, accounting for 63% of the total area in the LP under the SSP119 scenario, and 61% of total area in the LP under the SSP585 scenario. (Table S2). Although the spatiotemporal distribution of each vegetation type in the future period (2081–2100) was analogous to that of the historical period (2001–2020), conversions among the vegetation types occurred from the historical to the future period (Figure 3). The most noteworthy conversions were projected to occur at the end of the century (Table 2). Compared with 2001–2020, the area proportion of the shrub and grass was predicted to be transformed into forest accounted for more than 1% of the total area in the LP and mainly distributed in the Lvliang and Taihang Mountains under the SSP119 scenario during 2081–2100. In contrast, the area proportions of the forest, shrub and bare land were predicted to be transformed into grass accounted for 8%, 6%, and 76% of the total area in the LP during 2081–2100 under the same scenario. Under the SSP585 scenario during 2081–2100, all bare land in the Western high-altitude area was predicted to be transformed into grass, and the area proportion of the shrub and grass was predicted to be transformed into forest accounted for more than 1% of the total area in the LP, respectively. These conversions of vegetation types from the historical period to future period suggest that future climate change will influence the spatiotemporal distributions of vegetation types.

Table 2. Proportion (%) of vegetation type conversion area in the total area of the Loess Plateau from 2001–2020 to 2081–2100.

Vegetation Type	SSP119 Scenario				SSP585 Scenario			
	Forest	Shrub	Grass	Bare Land	Forest	Shrub	Grass	Bare Land
Forest	92	-	8	-	>99	-	<1	-
Shrub	2	92	6	-	3	97	<1	-
Grass	1	-	99	<1	3	<1	97	-
Bare Land	-	-	76	24	<1	-	>99	<1

3.2. Spatiotemporal Variations of Vegetation Ecological Functions

Compared with 2001–2020, the CS is a downward trend under the SSP119 scenario and on the rise under the SSP585 scenario during 2021–2100 (Figure 4a), while the SC and WC during 2021–2100 fluctuate considerably, with an overall upward trend 2021–2100 (Figure 4b,c).

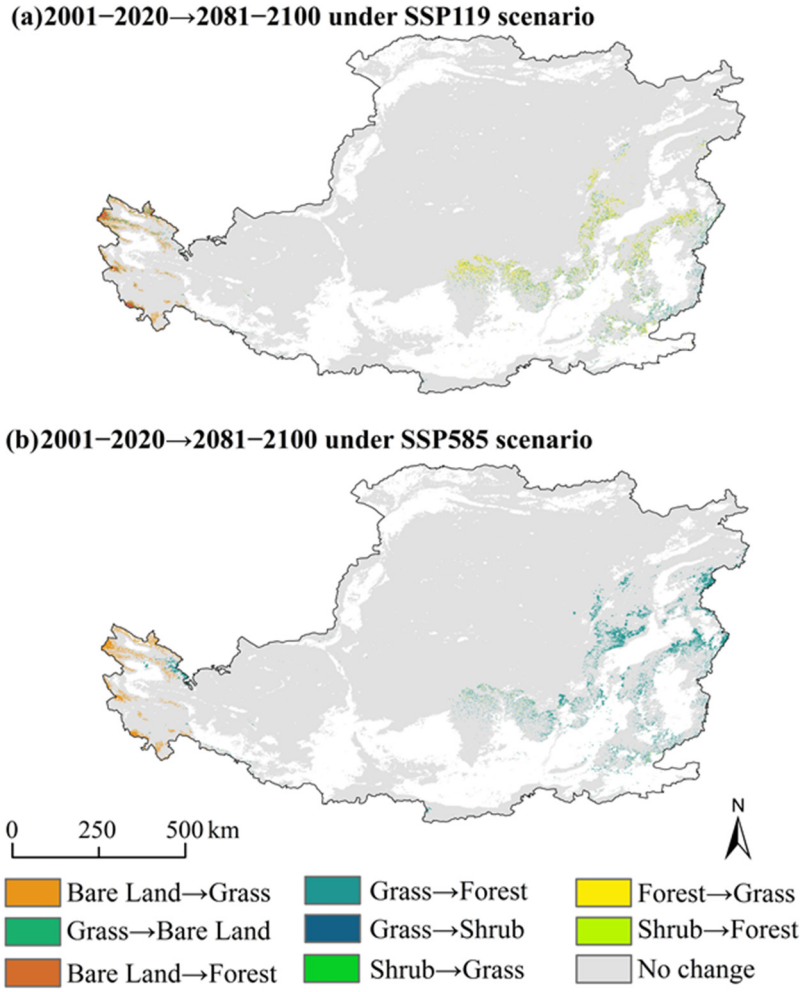


Figure 3. Conversions of vegetation types from 2001–2020 to 2081–2100.

During 2081–2100, the CS decreased from the southeastern region to the northwestern region, with the average CS being 8.78–14.20 tC·ha^{-1} (Figure S2(a1,a2), Table S3). Compared with 2001–2020, the average CS during the 2081–2100 period was projected to decrease by 0.32 tC·ha^{-1} under the SSP119 scenario and increase 5.14 tC·ha^{-1} under the SSP585 scenario. The regions predicted to experience a decrease were mainly distributed in the central and southeastern regions of the LP (Figure 5(a2,a3), Table 3). During 2081–2100, the SC decreased from the southeastern region to the northwestern region, with the average SC being 251.68–297.70 t·ha^{-1} (Figure S2(b1,b2), Table S3). Compared with 2001−2020, the average SC during the 2081–2100 period was projected to increase by 89.55–135.57 t·ha^{-1}. The regions of future increase were distributed everywhere except the western region (Figure 5(b2,b3), Table 3). During 2081–2100, the WC decreased from the southeast to the northwest, with the average WC being 117.67–134.39 mm (Figure S2(c1,c2), Table S3). Compared with 2001–2020, the average WC was projected to increase by 29.58–46.3 mm during 2081–2100. The regions of the decrease were mainly concentrated in the Qilian, Wushaoling, Xinglong, and Liupan Mountains (Figure 5(c2,c3), Table 3), and those of future increase were mainly distributed in the other regions of the LP. These results imply that future climate change will have a large impact on the ecological functions of vegetation in the LP.

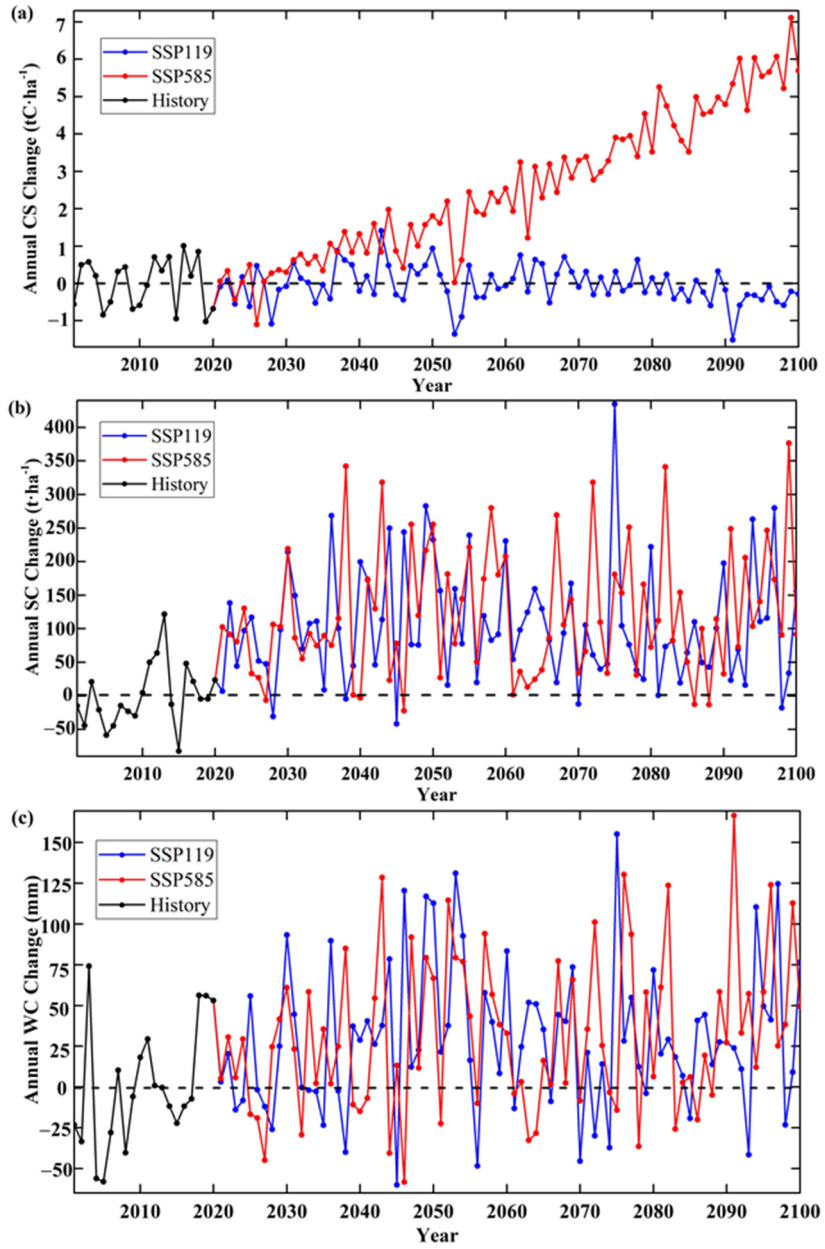


Figure 4. Change in the annual ecological functions of the Loess Plateau from 2001–2020 to 2021–2100. (**a**) Carbon stock function, CS; (**b**) soil conservation function, SC; and (**c**) water conservation function, WC.

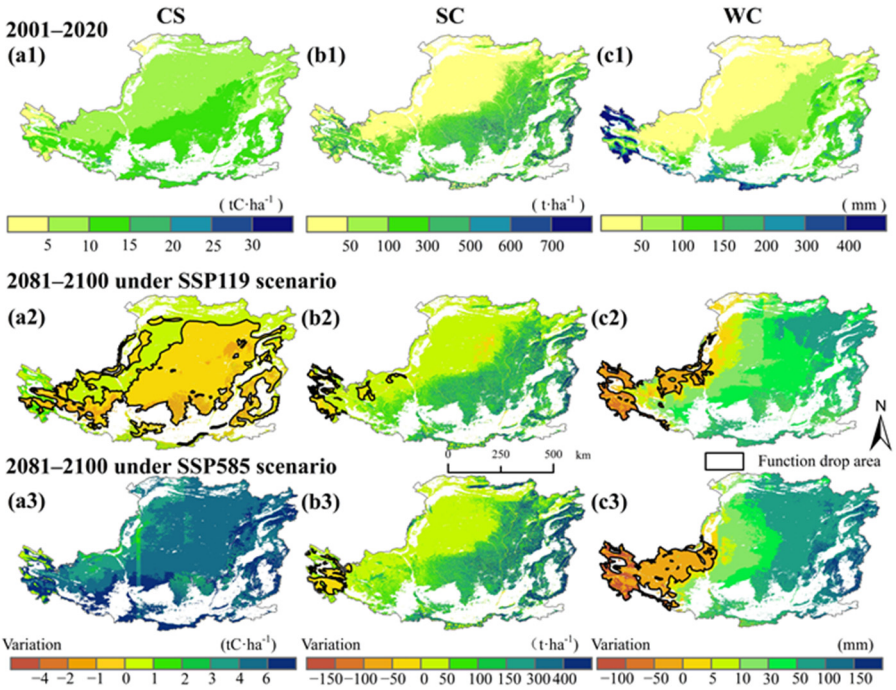


Figure 5. Spatiotemporal distribution during 2001–2020 and changes during 2081–2100 relative to 2001–2020 in the CS, SC, and WC of the Loess Plateau. Note: carbon stock function, CS; soil conservation function, SC; water conservation function, WC. (**a1**): the spatiotemporal distribution of the CS during 2001–2020; (**a2**,**a3**): the changes of the CS during 2081–2100 relative to 2001–2020 under SSP119 and SSP585 scenarios; (**b1**): the spatiotemporal distribution of the SC during 2001–2020; (**b2**,**b3**): the changes of the SC during 2081–2100 relative to 2001–2020 under SSP119 and SSP585 scenarios; (**c1**): the spatiotemporal distribution of the WC during 2001–2020; (**c2**,**c3**): the changes of the WC during 2081–2100 relative to 2001–2020 under SSP119 and SSP585 scenarios.

Table 3. Spatial statistical information on the changes in the CS, SC, and WC of the Loess Plateau during 2081–2100 relative to 2001–2020.

	SSP119 Scenario			SSP585 Scenario		
	CS	**SC**	**WC**	**CS**	**SC**	**WC**
Min	−4.99	−398.4	−127.54	−0.05	−274.7	−214.79
Max	4.13	3866.04	167.45	14.63	4740.09	327.23
Mean	−0.32	89.55	29.58	5.14	135.57	46.3
Std	0.7	132.01	30.19	1.64	203.92	53.51
AR (%)	47	4	8	<1	3	13

Note: Min, Max, Mean, Std, and AR indicate the minimum, maximum, mean, standard deviation, and the ratio of functional decline area of the Loess Plateau, respectively. Carbon stock function, CS ($tC \cdot ha^{-1}$); soil conservation function, SC ($t \cdot ha^{-1}$); water conservation function, WC (mm).

3.3. Synergistic and Trade-Off Relationships among Vegetation Ecological Functions

As shown in Figure 6, we overlapped the significant regions of the relationships between CS and WC (CSWC), SC and WC (SCWC), and CS and SC (CSSC), and obtained the regions where all three relationships are significant. During 2081–2100, the significant regions of the CS and WC trade-off relationship, the SC and WC synergistic relationship, and the CS and SC synergistic relationship were mainly distributed in the Liupan Mountain, Ordos Plateau and accounted for 9% of the total area in the LP (Figure 6b). During same period under the SSP585 scenario, the significant regions of the CS and WC synergistic relationship, the SC and WC trade-off relationship, the CS and SC synergistic relationship were mainly distributed in the eastern edge of Qilian Mountains, Mu Us Sandy Land and accounted for 3% of the total area in the LP (Figure 6c). In addition, compared with

2001–2020, the area with significant trade-offs between CS and WC would shrink under the SSP119 scenario and that with significant synergisms would expand under the SSP585 scenario during 2081–2100 (Figure S3(a1–a3)). Compared with 2001–2020, the area with significant synergisms between SC and WC would expand under the SSP119 scenario and that with significant trade-offs would expand under the SSP585 scenario during 2081–2100 (Figure S3(b1–b3)). Compared with 2001–2020, the area with significant synergistic relationships between CS and SC would shrink under both the SSP119 and SSP585 scenarios during 2081–2100 (Figure S3(c1–c3)). These results suggest that future climate change will vastly shift the trade-offs and synergies between ecological functions.

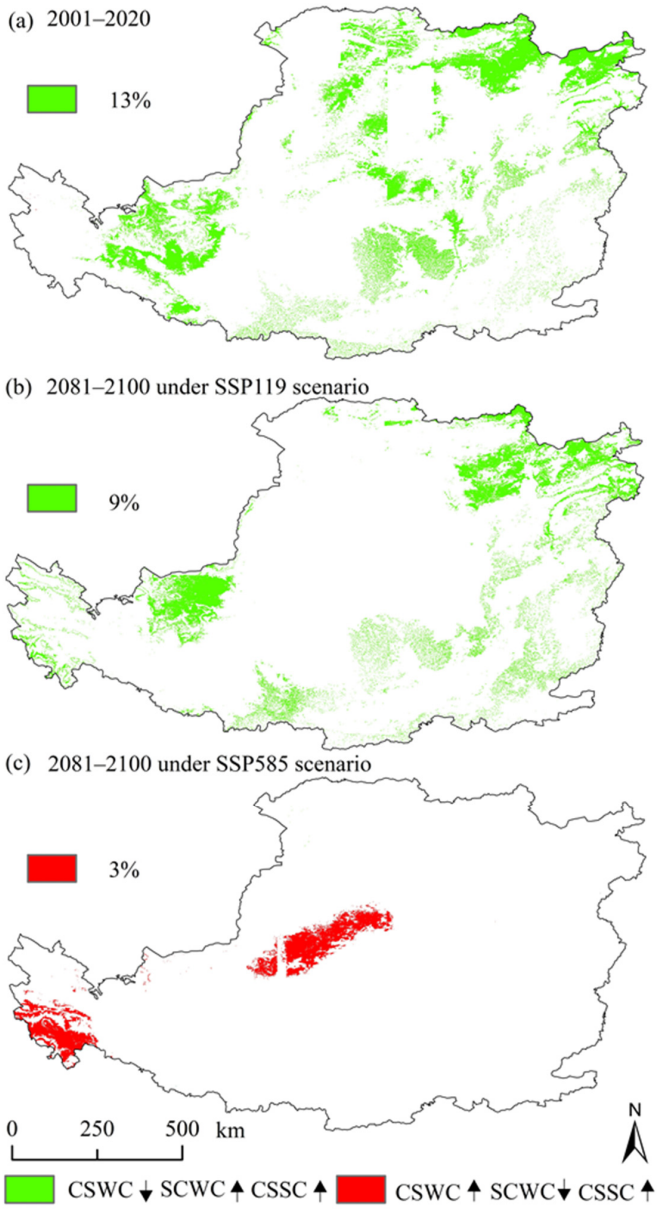


Figure 6. Significant trade-offs and synergistic relationships between the ecological functions of vegetation during 2001–2020 and 2081–2100. Note: carbon stock and water conservation functions, CSWC; soil conservation and water conservation functions, SCWC; carbon stock and soil conservation functions, CSSC; ↑significant synergism; ↓significant trade-off. (**a**): the significant trade-offs and synergistic relationship between the CSWC, SCWC, and CSSC during 2001–2020; (**b**): the significant trade-offs and synergistic relationship between the CSWC, SCWC, and CSSC during 2081–2100 under SSP119 scenario; (**c**): the significant trade-offs and synergistic relationship between the CSWC, SCWC, and CSSC during 2081–2100 under SSP585 scenario.

4. Discussion

At present, many studies on future ecological functions under climate change have been conducted worldwide [5–7]. However, these studies do not involve a particularly fine simulation of vegetation carbon and water flux and its structure, so the results are subject to considerable uncertainty. It is also difficult to achieve sustainable and efficient vegetation management and restoration plans. Therefore, this study addresses this knowledge gap by applying process-based dynamic vegetation models and high-resolution climate data to simulate and analyze the dynamic responses of ecological functions of vegetation to climate change in the LP.

Compared with 2001–2020, the area converted from shrub and grass into forest land by 2081–2100 was modeled to be mainly distributed in the Lvliang and Taihang Mountains (Figure 3), and this conversion was mainly caused by climate warming and drought [32]. The bare land in the western area was projected to be converted to grass, and the proportion of bare land area decreased or even disappeared. These phenomena are explained by plant community conversion due to climate change [32]. Previous studies reported that although temperature and precipitation on the LP will increase in the future, the evaporation caused by temperature increase will be greater than the precipitation, leading to a dry climate in the future [28]. These climate changes would advance the conversion of forest, shrub, and grass vegetation. The conversion of vegetation types from the historical to the future periods means that future climate change will greatly affect the spatiotemporal distribution of the vegetation. Predicting shifts in vegetation types can help make vegetation management in an area more targeted and efficient. For example, in the Lvliang and Taihang Mountains, proper thinning management or pruning could support vegetation growth. In the high elevations of the west, grazing may be appropriate.

The simulated trends of CS, SC, and WC in the future period under the two scenarios were quite different (Figure 4a–c). The reason is that we used scenarios with high and low forcing and greenhouse gas emissions to predict future ecological functions, and these scenarios included a range of possible future climatic changes such as temperature, precipitation, radiation, and carbon dioxide concentrations. The SSP119 scenario is represented by a low temperature, with the temperature rise in this century controlled at 1–2.4 °C and low atmospheric CO_2 concentrations. Under the SSP585 scenario, the temperature increase by the end of the century would be 2.8–5.7 °C. This leads to very different outcomes for the two future scenarios, and it is an approach that is often considered in current research aimed at predicting the future period [29,43,44].

The distributions of the CS, SC, and WC of the LP on the historical period were consistent with the results of existing research simulated by the InVEST model (Figure 5(a1,b1,c1)) [45,46], specifically that the spatiotemporal distribution of the ecological functions is affected by the hydrothermal conditions of the LP. During 2081–2100, the CS of the LP was high in the southeast and low in the northwest, with the CS being the lowest in the west at Qilian Mountain owing to the sparse vegetation in this region (Figure S2(a1,a2)). Under the SSP119 scenario, the CS in the central and southeastern regions of the LP in 2081–2100 decreased compared with 2001–2020, but the CS in the central and southeastern parts of the LP in 2081–2100 was still greater than that of the northwest (Figure 5(a2)) because the precipitation in the southeast was higher than that in the northwest. There is a notable positive correlation between precipitation and the CS [47]. The distribution of the SC on the LP was higher in the southeast and lower in the northwest (Figure S2(b1,b2)). The main reason for this phenomenon was the effect of precipitation in the future period. The distribution of precipitation in the LP is consistent with that in China, decreasing from southeast to northwest and generally tending to be warm and dry. Climatic zones migrate southward, resulting in corresponding changes in the vegetation zones. Under the SSP119 and SSP585 scenarios, the decline of SC caused by the vegetation in the western region (Figure 5(b2,b3)) is caused by the decrease in precipitation and an uneven seasonal distribution in this area. Every year, the months of July, August, and September are prone to heavy rain, aggravating the soil erosion in the region. Therefore, vegetation management

in this region should be strengthened. For example, such measures could include planting suitable vegetation with a scientific approach (e.g., *Haloxylon ammodendris*, sea-buckthorn, and other plants to enhance soil conservation ability) [48], implementing technical measures to make full use of the precipitation resources, and enhancing people's awareness of ecological protection [49]. The WC of the LP shows a high in the southeast and low in the northwest pattern, with the WC being highest in the western region (Figure S2(c1,c2)) owing to the high rainfall. Rainfall and evapotranspiration are important parameters for quantifying water production [50]. Precipitation minus evapotranspiration includes the soil moisture and possible runoff, and a drop in the WC indicates a possible water shortage. The western part of the LP has a high altitude and sufficient evapotranspiration. Compared with 2001–2020, the WC of the western part of the LP will decrease during 2081–2100 (Figure 5(c2,c3)). As a result, the amount of water resources in the high elevations of the west will decline and face the risk of water shortages.

The trade-offs and synergies among the CS, WC, and SC of the LP were determined by the climatic conditions of the region, including temperature and rainfall [51]. Changes in the carbon and water fluxes and the structure of the vegetation simulated by the dynamic vegetation model can capture the transformation of the relationship between ecological functions at the same site (Figures S3 and 6). To promote the sustainable management of regional ecosystems, we should consider the relationship between ecological functions, minimize trade-offs, and increase synergies. Ma et al. [52] showed that multiple ecosystem services can be gained by adjusting the ratios of forest, shrub, and grass vegetation simultaneously. The development of mixed forest can improve CS and SC. Strengthening natural grass protection, sustainable grazing, and reducing human disturbance can reduce the vulnerability of the ecological environment.

The current research methods for the study of ecological functions do not consider certain dynamic information on vegetation. However, the dynamic vegetation model can capture the dynamic changes in the carbon and water flux and the structure of the vegetation, especially under scenarios of future climate change. Combined with the equation for calculating the ecological functions of vegetation, the dynamic evolution of the ecological functions under climate change is accurately described, which provides a reference for the research of related subject. Therefore, studying the dynamic response of ecological functions of vegetation to climate change based on the LPJ-GUESS model can be used to carry out similar research in other regions of the world and obtain corresponding results. The LPJ-GUESS model has many vegetation parameters, so it is difficult to calibrate all the parameters. Therefore, this study only calibrated 21 sensitive parameters based on existing studies [34]. In future research, the simulation accuracy of the model needs to be further improved.

5. Conclusions

Studying the dynamic responses of the ecological functions of vegetation to climate change in the LP will help in the development of vegetation restoration and management strategies to adapt to climate change and provide guarantees for ecological protection and high-quality development in the region. The process-based dynamic vegetation model to simulate the ecological functions of ecologically fragile areas will effectively improve vegetation management restoration projects. Taking the LP as a case study area, this study used the dynamic vegetation model to simulate the ecological functions of vegetation. The results showed that near the end of the century, the shrub and grass vegetation in the Lvliang and Taihang Mountains will be transformed into forest, and the bare land in the Western high-altitude areas will be transformed into grass. Furthermore, the distribution of CS, SC, and WC of the LP were high in the southeast and low in the northwest, with the CS of the Qilian Mountain in the west being the lowest and the WC being the highest. The significant relationships among the CS, SC, and WC under the SSP119 scenario were mainly concentrated in the Liupan Mountains and the Ordos Plateau, accounting for 9% of the LP. The significant relationships among CS, SC, and WC under the SSP585 scenario were

mainly concentrated at the eastern edge of the Qilian Mountains and the Mu Us Sandy Land, accounting for 3% of the LP. These results are helpful for the establishment of vegetation restoration and management strategies on the LP. The approach proposed in this study could provide a reference for the study of other ecologically fragile regions worldwide.

Supplementary Materials: The following supporting information can be downloaded at: https://www.mdpi.com/article/10.3390/f13091464/s1. Figure S1: Spatiotemporal distribution of each vegetation type during 2001–2020 and 2081–2100; Figure S2: Spatiotemporal distributions of CS, SC, and WC on the Loess Plateau during 2081–2100; Figure S3: Spatiotemporal patterns of the relationships between CSWC, SCWC, and CSSC during 2001–2020 and 2081–2100. Table S1: The 21 sensitive parameters in the LPJ-GUESS model and their interpretations; Table S2: Proportion (%) of the area with each vegetation type in the total area of the Loess Plateau during 2001–2020 and 2081–2100; Table S3: Spatiotemporal distributions of the CS, SC, and WC on the Loess Plateau during 2001–2020 and 2081–2100.

Author Contributions: Conceptualization, Y.S. and S.P.; methodology, S.P. and Y.D.; software, S.P.; validation, Y.S.; formal analysis, Y.S.; investigation, Y.S.; resources, S.P.; data curation, Y.S.; writing—original draft preparation, Y.S.; writing—review and editing, Y.S., J.Z., S.P. and Y.D.; visualization, Y.S.; supervision, S.P.; project administration, S.P.; funding acquisition, S.P. All authors have read and agreed to the published version of the manuscript.

Funding: This research was funded by the National Natural Science Foundation of China, grant number 42077451; the Natural Science Foundation of Shaanxi Province, China, grant number 2020JQ-418; and the Key R & D project of Ningxia Hui Autonomous Region, grant number 2020BCF01001.

Conflicts of Interest: The authors declare no conflict of interest.

References

1. Daily, G.C. Nature's services: Societal dependence on natural ecosystems (1997). In *The Future of Nature*; Yale University Press: New Haven, CT, USA, 2013; pp. 454–464. [CrossRef]
2. Simonit, S.; Perrings, C. Sustainability and the value of the 'regulating' services: Wetlands and water quality in Lake Victoria. *Ecol. Econ.* **2011**, *70*, 1189–1199. [CrossRef]
3. Yang, D.; Liu, W.; Tang, L.Y.; Chen, L.; Li, X.Z.; Xu, X.L. Estimation of water provision service for monsoon catchments of South China: Applicability of the InVEST model. *Landsc. Urban Plan.* **2019**, *182*, 133–143. [CrossRef]
4. Engelbrecht, B.M.J. Plant ecology: Forests on the brink. *Nature* **2012**, *491*, 675–676. [CrossRef] [PubMed]
5. Zhao, M.M.; He, Z.B.; Du, J.; Chen, L.F.; Lin, P.F.; Fang, S. Assessing the effects of ecological engineering on carbon storage by linking the CA-Markov and InVEST models. *Ecol. Indic.* **2019**, *98*, 29–38. [CrossRef]
6. Xiang, M.S.; Yang, J.; Li, W.H.; Song, Y.T.; Wang, C.J.; Liu, Y.; Liu, M.L.; Tan, Y.X. Spatiotemporal Evolution and Simulation Prediction of Ecosystem Service Function in the Western Sichuan Plateau Based on Land Use Changes. *Front. Environ. Sci.* **2022**, *10*, 391. [CrossRef]
7. Zhu, G.F.; Qiu, D.D.; Zhang, Z.A.X.; Sang, L.Y.; Liu, Y.W.; Wang, L.; Zhao, K.L.; Ma, H.Y.; Xu, Y.X.; Wan, Q.Z. Land-use changes lead to a decrease in carbon storage in arid region, China. *Ecol. Indic.* **2021**, *127*, 107770. [CrossRef]
8. Liang, Y.; Hashimoto, S.; Liu, L. Integrated assessment of land-use/land-cover dynamics on carbon storage services in the Loess Plateau of China from 1995 to 2050. *Ecol. Indic.* **2021**, *120*, 106939. [CrossRef]
9. Fisher, J.B.; Huntzinger, D.N.; Schwalm, C.R.; Sitch, S. Modeling the Terrestrial Biosphere. *Annu. Rev. Environ. Resour.* **2014**, *39*, 91–123. [CrossRef]
10. Logsdon, R.A.; Chaubey, I. A quantitative approach to evaluating ecosystem services. *Ecol. Model.* **2013**, *257*, 57–65. [CrossRef]
11. Lavorel, S.; Bayer, A.; Bondeau, A.; Lautenbach, S.; Ruiz-Frau, A.; Schulp, N.; Seppelt, R.; van Verburg, P.; Teeffelen, A.; Vannier, C.; et al. Pathways to bridge the biophysical realism gap in ecosystem services mapping approaches. *Ecol. Indic.* **2017**, *74*, 241–260. [CrossRef]
12. Smith, B.; Prentice, I.C.; Sykes, M.T. Representation of vegetation dynamics in the modelling of terrestrial ecosystems: Comparing two contrasting approaches within European climate space. *Glob. Ecol. Biogeogr.* **2001**, *10*, 621–637. [CrossRef]
13. Sitch, S.; Smith, B.; Prentice, I.C.; Arneth, A.; Bondeau, A.; Cramer, W.; Kaplan, J.O.; Levis, S.; Lucht, W.; Sykes, M.T.; et al. Evaluation of ecosystem dynamics, plant geography and terrestrial carbon cycling in the LPJ dynamic global vegetation model. *Glob. Change Biol.* **2003**, *9*, 161–185. [CrossRef]
14. Sato, H.; Itoh, A.; Kohyama, T. SEIB-DGVM: A new dynamic global vegetation model using a spatially explicit individual-based approach. *Ecol. Model.* **2007**, *200*, 279–307. [CrossRef]

15. Smith, B.; Warlind, D.; Arneth, A.; Hickler, T.; Leadley, P.; Siltberg, J.; Zaehle, S. Implications of incorporating N cycling and N limitations on primary production in an individual-based dynamic vegetation model. *Biogeosciences* **2014**, *11*, 2027–2054. [CrossRef]
16. Hickler, T.; Vohland, K.; Feehan, J.; Miller, P.A.; Smith, B.; Costa, L.; Giesecke, T.; Fronzek, S.; Carter, T.R.; Cramer, W.; et al. Projecting the future distribution of European potential natural vegetation zones with a generalized, tree species-based dynamic vegetation model. *Glob. Ecol. Biogeogr.* **2012**, *21*, 50–63. [CrossRef]
17. Peng, S.Z.; Li, Z. Incorporation of potential natural vegetation into revegetation programmes for sustainable land management. *Land Degrad. Dev.* **2018**, *29*, 3503–3511. [CrossRef]
18. Usman, H.; Pugh, T.A.M.; Ahlstrom, A.; Baig, S. Climate change projections of terrestrial primary productivity over the Hindu Kush Himalayan forests. *Earth Syst. Dyn.* **2021**, *12*, 857–870. [CrossRef]
19. Liang, S.Q.; Peng, S.Z.; Chen, Y.M. Carbon Cycles of Forest Ecosystems in a Typical Climate Transition Zone under Future Climate Change: A Case Study of Shaanxi Province, China. *Forests* **2019**, *10*, 1150. [CrossRef]
20. Cao, S.X.; Chen, L.; Shankman, D.; Wang, C.M.; Wang, X.B.; Zhang, H. Excessive reliance on afforestation in China's arid and semi-arid regions: Lessons in ecological restoration. *Earth-Sci. Rev.* **2011**, *104*, 240–245. [CrossRef]
21. Feng, X.M.; Fu, B.J.; Piao, S.; Wang, S.H.; Ciais, P.; Zeng, Z.Z.; Lu, Y.H.; Zeng, Y.; Li, Y.; Jiang, X.H.; et al. Revegetation in China's Loess Plateau is approaching sustainable water resource limits. *Nat. Clim. Change* **2016**, *6*, 1019–1022. [CrossRef]
22. Liu, S.Y.; Hu, N.K.; Zhang, J.; Lv, Z.C. Spatiotemporal change of carbon storage in the Loess Plateau of northern Shaanxi, based on the InVEST Model. *Sci. Cold Arid. Reg.* **2018**, *10*, 240–250. [CrossRef]
23. Lv, X.; Zuo, Z.; Xiao, P. Evaluation of water conservation capacity of loess plateau typical mountain ecosystems based on InVEST model simulation. In *IOP Conference Series: Earth and Environmental Science*; IOP Publishing: Bristol, UK, 2017; Volume 69, p. 012030. [CrossRef]
24. Wang, X.; Wu, J.; Liu, Y.; Hai, X.; Shanguan, Z.; Deng, L. Driving factors of ecosystem services and their spatiotemporal change assessment based on land use types in the Loess Plateau. *J. Environ. Manag.* **2022**, *311*, 114835. [CrossRef] [PubMed]
25. Arowolo, A.O.; Deng, X.; Olatunji, O.A.; Obayelu, A.E. Assessing changes in the value of ecosystem services in response to land-use/land-cover dynamics in Nigeria. *Sci. Total Environ.* **2018**, *636*, 597–609. [CrossRef] [PubMed]
26. Dai, X.; Wang, L.; Huang, C.; Fang, L.; Wang, S.; Wang, L. Spatiotemporal variations of ecosystem services in the urban agglomerations in the middle reaches of the Yangtze River, China. *Ecol. Indicat.* **2020**, *115*, 106394. [CrossRef]
27. Xu, X.; Yang, G.; Tan, Y.; Liu, J.; Hu, H. Ecosystem services trade-offs and determinants in China's Yangtze River economic belt from 2000 to 2015. *Sci. Total Environ.* **2018**, *634*, 1601–1614. [CrossRef]
28. Peng, S.Z.; Gang, C.C.; Cao, Y.; Chen, Y.M. Assessment of climate change trends over the Loess Plateau in China from 1901 to 2100. *Int. J. Climatol.* **2018**, *38*, 2250–2264. [CrossRef]
29. He, X.B.; Li, Z.B.; Hao, M.D.; Tang, K.L.; Zheng, F.L. Down-scale analysis for water scarcity in response to soil-water conservation on Loess Plateau of China. *Agric. Ecosyst. Environ.* **2003**, *94*, 355–361. [CrossRef]
30. Chen, M.; Zhang, X.; Li, M.; Zhang, J.; Cao, Y. Climate-growth pattern of Pinus tabulaeformis plantations and their resilience to drought events in the Loess Plateau. *For. Ecol. Manag.* **2021**, *499*, 119642. [CrossRef]
31. Shi, H.; Shao, M.G. Soil and water loss from the Loess Plateau in China. *J. Arid. Environ.* **2000**, *45*, 9–20. [CrossRef]
32. Han, Q.G.; Ding, Y.X.; Peng, S.Z. Sustainable and cost-effective vegetation restoration framework under climate change. *For. Ecol. Manag.* **2021**, *496*, 119436. [CrossRef]
33. Riahi, K.; van Vuuren, D.P.; Kriegler, E.; Edmonds, J.; O'Neill, B.C.; Fujimori, S.; Bauer, N.; Calvin, K.; Dellink, R.; Fricko, O.; et al. The Shared Socioeconomic Pathways and their energy, land use, and greenhouse gas emissions implications: An overview. *Glob. Environ. Change* **2017**, *42*, 153–168. [CrossRef]
34. Bagnara, M.; Gonzalez, R.S.; Reifenberg, S.; Steinkamp, J.; Hickler, T.; Werner, C.; Dormann, C.F.; Hartig, F. An R package facilitating sensitivity analysis, calibration and forward simulations with the LPJ-GUESS dynamic vegetation model. *Environ. Model. Softw.* **2019**, *111*, 55–60. [CrossRef]
35. Santhi, C.; Arnold, J.G.; Williams, J.R.; Dugas, W.A.; Srinivasan, R.; Hauck, L.M. Validation of the swat model on a large rwer basin with point and nonpoint sources 1. *J. Am. Water Resour. Assoc.* **2001**, *37*, 1169–1188. [CrossRef]
36. Wolf, A.; Callaghan, T.V.; Larson, K. Future changes in vegetation and ecosystem function of the Barents Region. *Clim. Change* **2008**, *87*, 51–73. [CrossRef]
37. Zhang, K.; Lv, Y.H.; Fu, B.J. Vegetation restoration and its influences on ecosystem services in areas typical of the Loess Plateau. *J. Ecol. Rural. Environ.* **2017**, *33*, 23–31. [CrossRef]
38. Jiang, C.; Zhang, H.Y.; Tang, Z.P.; Labzovskii, L. Evaluating the coupling effects of climate variability and vegetation restoration on ecosystems of the Loess Plateau, China. *Land Use Policy* **2017**, *69*, 134–148. [CrossRef]
39. Cai, C.F.; Ding, S.W.; Shi, Z.H.; Huang, L.; Zhang, G.Y. Study of applying USLE and geographical information system IDRISI to predict soil erosion in small watershed. *J. Soil Water Conserv.* **2000**, *14*, 19–24. [CrossRef]
40. Zhao, J.; Li, J.; Liu, Q.H.; Xu, B.D.; Yu, W.T.; Lin, S.R.; Hu, Z. Estimating fractional vegetation cover from leaf area index and clumping index based on the gap probability theory. *Int. J. Appl. Earth Obs. Geoinf.* **2020**, *90*, 102112. [CrossRef]
41. Wei, H.J.; Fan, W.G.; Ding, Z.Y.; Weng, B.Q.; Xing, K.X.; Wang, X.C.; Lu, N.C.; Ulgiati, S.; Dong, X.B. Ecosystem Services and Ecological Restoration in the Northern Shaanxi Loess Plateau, China, in Relation to Climate Fluctuation and Investments in Natural Capital. *Sustainability* **2017**, *9*, 199. [CrossRef]

42. Zhang, Y.; Liu, Y.F.; Zhang, Y.; Liu, Y.; Zhang, G.X.; Chen, Y.Y. On the spatial relationship between ecosystem services and urbanization: A case study in Wuhan, China. *Sci. Total Environ.* **2018**, *637*, 780–790. [CrossRef]
43. Popp, A.; Calvin, K.; Fujimori, S.; Havlik, P.; Humpenöder, F.; Stehfest, E. Land-use futures in the shared socio-economic pathways. *Glob. Environ. Change* **2017**, *42*, 331–345. [CrossRef]
44. Xi, Y.; Peng, S.; Liu, G.; Ducharne, A.; Ciais, P.; Prigent, C.; Tang, X. Trade-off between tree planting and wetland conservation in China. *Nat. Commun.* **2022**, *13*, 1967. [CrossRef]
45. Zhao, X.Y.; Ma, P.Y.; Li, W.Q.; Du, Y.X. Spatiotemporal changes of supply and demand relationships of ecosystem services in the Loess Plateau. *J. Geogr.* **2021**, *76*, 2780–2796. [CrossRef]
46. Wang, X.Z.; Wu, J.Z.; Wu, P.X.; Shangguan, Z.P.; Deng, L. Spatial and temporal distribution and trade-off of water conservation, soil conservation and NPP services in the ecosystems of the Loess Plateau from 2000 to 2015. *J. Soil Water Conserv.* **2021**, *35*, 114–121.
47. Jiang, C.; Zhang, H.Y.; Wang, X.C.; Feng, Y.Q.; Labzovskii, L. Challenging the land degradation in China's Loess Plateau: Benefits, limitations, sustainability, and adaptive strategies of soil and water conservation. *Ecol. Eng.* **2019**, *127*, 135–150. [CrossRef]
48. Li, X.; Yu, X.; Wu, K.N.; Feng, Z.; Liu, Y.N.; Li, X.L. Land-use zoning management to protecting the Regional Key Ecosystem Services: A case study in the city belt along the Chaobai River, China. *Sci. Total Environ.* **2021**, *762*, 143167. [CrossRef]
49. DENG, L.; SHANGGUAN, Z.P. High quality developmental approach for soil and water conservation and ecological protection on the loess plateau. *Front. Agric. Sci. Eng.* **2021**, *8*, 501–511. [CrossRef]
50. Su, C.H.; Dong, M.; Fu, B.J.; Liu, G.H. Scale effects of sediment retention, water yield, and net primary production: A case-study of the Chinese Loess Plateau. *Land Degrad. Dev.* **2020**, *31*, 1408–1421. [CrossRef]
51. Jiang, C.; Zhang, H.; Zhang, Z. Spatially explicit assessment of ecosystem services in China's Loess Plateau: Patterns, interactions, drivers, and implications. *Glob. Planet. Change* **2018**, *161*, 41–52. [CrossRef]
52. Ma, S.; Qiao, Y.P.; Wang, L.J.; Zhang, J.C. Terrain gradient variations in ecosystem services of different vegetation types in mountainous regions: Vegetation resource conservation and sustainable development. *For. Ecol. Manag.* **2021**, *482*, 118856. [CrossRef]